Available online at www.sciencedirect.com
SCIENCE DIRECT®
ELSEVIER
Journal of Magnetism and Magnetic Materials 292 (2005) 89–99
Journal of magnetism and magnetic materials
www.elsevier.com/locate/jmmm

Magnetization, shape memory and hysteresis behavior of single and polycrystalline FeNiCoTi

H. Sehitoglu[a,*], C. Efstathiou[a], H.J. Maier[b], Y. Chumlyakov[c]

[a] *Mechanical and Industrial Engineering, University of Illinois, 1206 West Green Street, Urbana, IL 61801, USA*
[b] *University of Paderborn, Lehrstuhl für Werkstoffkunde, 33095 Paderborn, Germany*
[c] *Tomsk State University, 1, Novo-Sobornay, 634050 Tomsk, Russia*

Received 22 November 2003; received in revised form 20 August 2004
Available online 11 November 2004

Abstract

We report on the shape memory characteristics and magnetic behavior of polycrystalline and single crystalline FeNiCoTi. Predeforming the samples in the martensitic state and biasing of the martensite variants produced anisotropy in the magnetization behavior allowing the 'easy axis' to be identified as the '*a*-axis' in the martensitic state. Based on these results, we provide an estimate of the magnetic anisotropy energy as 8.34×10^5 ergs/cm^3. The results confirm the different magnetization behavior in the martensitic and austenitic states, and the shift in transformation temperatures upon application of a magnetic field. Shape memory strains near 2.5% are demonstrated under constant stress temperature cycling and upon heating at zero stress after deformation. We present a thermodynamics based theory that explains the origin of the hysteresis in this class of alloys emanating from the dissipation of energy due to plastic deformation. We predict the thermal hysteresis (135 K), and the shift in transformation temperature (14 K) with applied magnetic fields in agreement with the experimental results. The possibility of utilizing these classes of alloys as magnetic shape memory alloys is discussed.

Keywords: Anisotropy; Magnetic shape memory; Energy dissipation

1. Introduction

The FeNiCoTi shape memory alloys undergo austenite to martensite transformation upon cooling to the martensite start temperature. The transformation is thermo-elastic, and upon heating the reverse transformation occurs at the austenite start temperature. Transformation strains as high as 2.5% are reported in the current study, which exceed previously reported values [1]. The FeNiCoTi based alloys transform from a cubic austenitic phase to a tetragonal martensitic phase. Based on the lattice parameters, the habit plane, the twinning shear and the transformation

*Corresponding author. Tel.: +1 217 333 4112; fax: +1 217 244 6534.
E-mail address: huseyin@uiuc.edu (H. Sehitoglu).

0304-8853/$ - see front matter © 2004 Elsevier B.V. All rights reserved.
doi:10.1016/j.jmmm.2004.10.101

strain as a function of orientation have been established [1]. These alloys can be optimized to produce shape memory behavior to suit specific applications. Since the FeNiCoTi alloys are also ferromagnetic the applied magnetic fields can influence the transformation shape memory behavior. Previous works have focused on deformation response of FeNiCoTi in polycrystalline form by research groups in Ukraine [2–4], Germany [5,6] and Japan [7]. The transformation strains in previous work were confined to less than 1% [6,8], and there has not been an investigation of thermal hysteresis under applied stress or under magnetic fields motivating a closer look at these issues. Our current work is focused on single crystals, and provides new insight on orientation dependence of magnetization under applied stress.

Our previous work [1] was conducted utilizing a 650 °C aging treatment, while in the current paper we focus on the 550 °C aging treatment of FeNiCoTi. The 550 °C aging treatment produces a finer precipitate structure, a higher martensite start temperature, and results in a narrower thermal hysteresis associated with the phase transformation. In the present paper, we report on the magnetization behavior upon changing the temperature, the shift in transformation temperatures upon application of an applied magnetic field, and the role of applying a tensile versus compressive deformation in the martensitic state on magnetization behavior. With applied deformation on [0 0 1] crystals, we subsequently measure the magnetic anisotropy produced by biasing of the variants. The experiments also investigate the magnetization behavior in [0 1 1] and [1 2 3] orientations and the polycrystalline material in both the martensitic and austenitic states.

The FeNiCoTi materials have potential as actuators and sensors. The current work builds upon our successful demonstration and analysis of large reversible strains due to phase transformations in FeNiCoTi alloys. One of the major advantages of these materials is that they exhibit significantly higher strength and higher ductility compared to the nickel–manganese–gallium ferromagnetic shape memory materials that have attracted considerable recent attention [9–11]. By using selected crystal orientations and textures, it would be easier to control temperature-, stress- and magnetic-induced shape memory in these classes of alloys. There is strong indication that both FeNiCoTi materials exhibit large magnetic anisotropy energy (the difference in magnetization—applied field behavior between easy and hard axis) to facilitate martensite variant motion under applied fields.

Since these materials will be used for applications involving stress and magnetic fields we present experimental results on thermal hysteresis. A theoretical treatment of the transformation hysteresis is also provided identifying the relaxation of internal energy as the source of the hysteresis in these classes of alloys. The model provides explicit expressions for the forward and reverse transformation temperatures incorporating the role of external stress, transformation strain, and the variant–variant interaction terms. The shift in the transformation temperatures with increasing applied magnetic field is also interpreted based on the thermodynamics of the transformation.

2. Motivation of the current study

The purpose of the work is three-fold:

(i) to demonstrate the magnitude of hysteresis in temperature cycling under stress and under magnetic fields, and explanation of the results based on mechanics models and microstructural observations,
(ii) to present experimental results displaying transformation strains of the order of 2.5% in FeNiCoTi polycrystals,
(iii) to illustrate magnetization behavior in austenitic and martensitic states, and different magnetization behavior between the easy and hard axis of the tetragonal martensite in FeNiCoTi providing an estimate of magnetic anisotropy energy.

3. Materials background

The FeNiCoTi alloys are a relatively new class of shape memory alloys. These materials are

unusual because they exhibit shape memory with an FCC austenitic structure, in contrast to NiTi and other well-known shape memory alloys, which have an ordered crystal structure in the austenitic regime. These alloys prove that shape memory can occur in FCC austenitic domains if considerable slip resistance exists typically through ultra fine precipitates. The lattice constants have been documented in the work of Koval et al. [9] who demonstrated that the c/a ratio in this material is larger than 1 where the c-axis and the a-axis define the crystal structure. If a tensile stress is applied to [0 0 1] crystals the variant with the c-axis vertical will be favored compared to other variants. On the other hand, if a compressive stress is applied to $\langle 001 \rangle$ crystals the variant with the a-axis vertical will be produced. The variant motion can be also accomplished with a magnetic field and such rearrangement can potentially produce large strains allowing actuation and sensing components.

The originally cast material with Fe–29Ni–18-Co–4Ti (weight%) composition was grown to single crystals using the Bridgman method. After single crystal growth, homogenization of the samples was undertaken at 1050 °C for 20 h followed by a water quench. The specimens were aged at 550 °C for 3 h to produce a fine precipitate structure with ordered particles ($L1_2-Ni_3Ti$ precipitates). A portion of the cast material was cold rolled and subjected to the same heat treatment as the single crystals.

Differential scanning calorimetry was utilized to establish the transformation temperatures as a function of aging treatment. The results are shown in Fig. 1. Upon cooling the martensite start temperature is reached near −75 °C for the 600 °C aging treatment and near −55 °C for the 550 °C treatment. Upon heating the austenitic start temperature is near 30 °C for all the heat treatments. The thermal hysteresis in these materials is near 135 °C, a value higher than observed for typical Ni- and Cu-based shape memory alloys. The thermal hysteresis represents the temperature differential between the forward and reverse martensitic transformation (DSC peak to peak measurement shown in Fig. 1). The texture of the polycrystals was established using X-ray

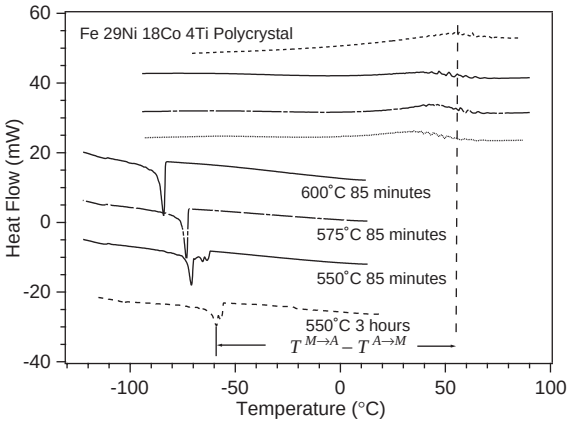

Fig. 1. Differential scanning calorimetry results displaying the transformation temperatures in FeNiCoTi as a function of aging treatment. The thermal hysteresis for the 550 °C 3 h treatment case is nearly 135 °C. The sample weight for the 550 °C 3 h case was 30 mg.

diffraction techniques, and inverse pole figures were generated from the diffraction data using popLA software [12]. The results are shown in Fig. 2 displaying that some preferential orientation in [1 1 1] and [1 0 1] directions exist, however the texture is not very strong. Since the results for transformation strains and magnetization are crystal orientation dependent, texture measurements for polycrystals provides the anisotropy information influencing the results.

In Fig. 3 the martensite plates are shown after constant stress thermal cycling. The martensite plates are shown as dark bands while the lighter background represents the austenite.

Because of thermal hysteresis a considerable martensite volume fraction can exist at room temperature and this is evident in Fig. 3(a). The residual martensite in FeNiCoTi produces internal stress fields that modify the shape memory characteristics by changing the austenite finish temperature, generating a two-way shape memory effect, and altering the stress levels for transformation. In Fig. 3(b) the martensite plate is internally twinned and the presence of dislocations in the form of loops emanating from the interface is evident. The presence of the dislocation loops produce a relaxation of the internal energy in the transforming domains and is primarily responsible

for hysteresis upon reverse transformation from martensite to austenite. Although there is recognition that hysteresis in all shape memory alloys is a significant consideration in design with these materials, the origins of the hysteresis has not been fully understood. This is the first time where a preliminary calculation for hysteresis is conducted on FeNiCoTi associated with dislocation formation at the austenite/martensite interfaces as a source of dissipative mechanism. This will be discussed further in a later section under '*Transformation Hysteresis*'.

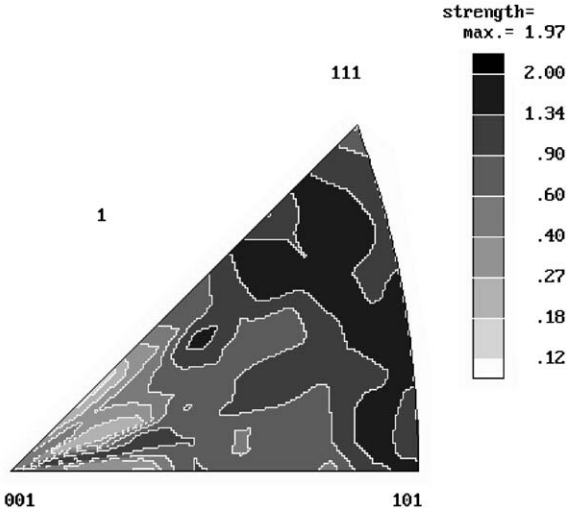

Fig. 2. Inverse pole figure obtained on polycrystalline samples displaying the presence of a small degree of texture with preference near [1 1 1] and [0 1 1] poles. The texture results are useful in interpretation of magnetization curves to be presented later.

4. Experimental techniques

The magnetization experiments are conducted with the Magnetic Property Measurement System produced by Quantum Design at the Materials Research Laboratory at the University of Illinois. It operates over a broad range of temperatures (2–400 K) and magnetic fields up to 7 T. The magnetic flux is measured with detection coil sensors as the sample is subjected to temperature and magnetic fields. Biasing the martensite variants was achieved via compression and tension tests. The tension specimens were electro-discharge machined from single crystal ingots to have a 4 mm gage section, 2 mm width and 1.5 mm thickness. The compression tests were performed on rectangular samples with dimensions of $10 \times 4 \times 4\,\mathrm{mm}^3$. The experiments were conducted on a servo-hydraulic Instron load frame via an

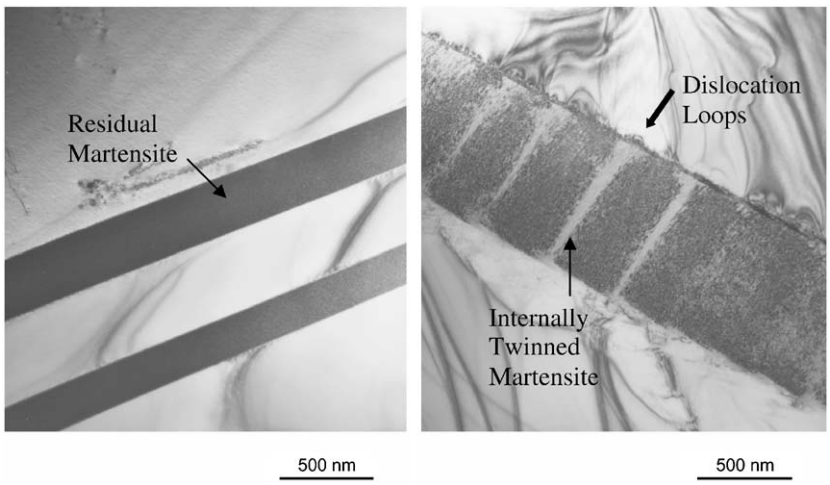

Fig. 3. (a) Transmission electron microscopy results displaying the residual martensite in samples subjected to reversible transformations, (b) evidence of dislocation generation at the austenite martensite interface (shown with an arrow). Internal twinning is evident in the martensite.

Instron controller through a LabVIEW interface. All of the strain–temperature curves were performed in stress control. Strain was measured directly on the sample using a miniature MTS extensometer with a 3 mm gage length.

The thermal cycling experiments were conducted using tension dog bone type specimens. In these experiments, the temperature was cycled between −175 to 175 °C. The duration of the heating and cooling was approximately 60 min per cycle to minimize transient effects and thermal gradients. The heating was accomplished with induction heating. Cooling was achieved by copper tubing that surrounds the specimen and grips and is fed with liquid nitrogen.

5. Experimental results

We first discuss the shape memory behavior of FeNiCoTi under constant stress thermal cycling. Upon cooling the strains increase in the tensile direction upon reaching the martensite start temperature. The experimental results for two cycles are shown in Fig. 4. When the temperature reaches near −120 °C the transformation strains saturate. Upon heating the reverse transformation initiates near 30 °C corresponding to the austenite start temperature and is nearly complete when the temperature exceeds 130 °C. Because the curves are highly nonlinear the hysteresis is defined at the midpoint of the loops as indicated in Fig. 4 with a horizontal arrow. The results are presented for three cycles in Fig. 4 and demonstrate that the transformation is reversible with a hysteresis of 135 °C.

Experimental results showing magnetization as a function of temperature are shown in Fig. 5. These results are given as a function of two applied magnetic fields, 4 T and 7 T, respectively. The results confirm the transformation temperatures observed in previous DSC and thermal cycling experiments. There is a shift in transformation temperatures with increasing field and this finding is consistent with the thermodynamics of the transformation as described later.

We note when the martensitic state is achieved upon cooling to below martensite start temperature multiple martensite variants form in a self-accommodating fashion. Upon application of stress one of the variants grow at the expense of the others producing a single variant of martensite. The single variant of martensite formed under compression and tension are different as expected.

After deformation, the specimens contain oriented martensite. In the FeNiCoTi alloy the *c*-axis of the tetragonal lattice is larger than the *a*-axis,

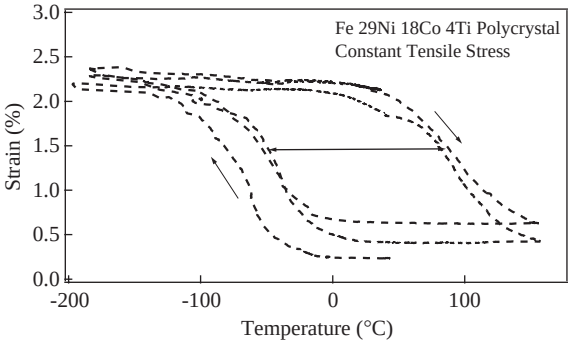

Fig. 4. Strain–temperature behavior under temperature cycling of FeNiCoTi under a constant tensile stress. The thermal hysteresis is shown with an arrow. The applied stress is 300 MPa in this case.

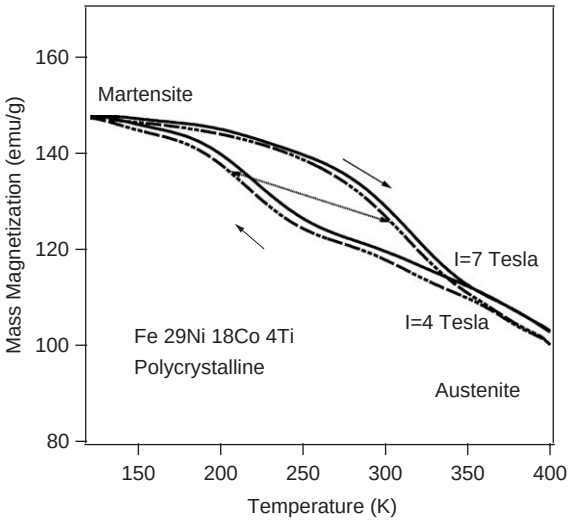

Fig. 5. The shift in transformation temperatures with increasing magnetic field. The increase in magnetic field from 4 to 7 T shifts the transformation temperatures. The transformation hysteresis is 100 °C in this case (shown with a line with arrow at both ends).

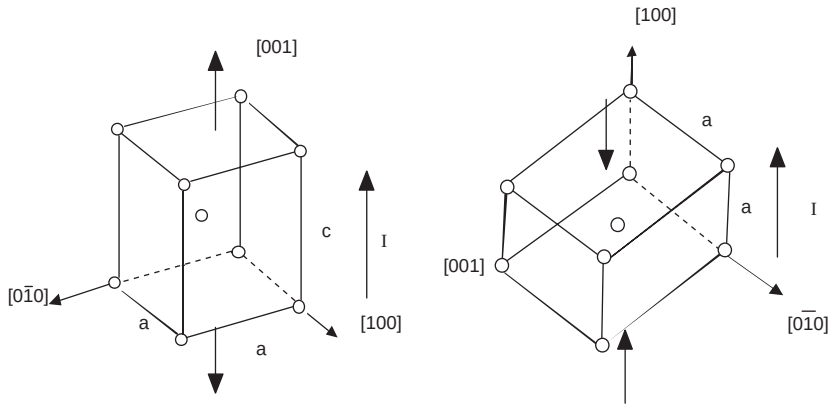

Fig. 6. The biasing of the martensite variants upon application of tension and compression respectively, *I* is the applied field direction (shown with the vertical vector). Note that under compression the variant with '*a* axis' vertical is preferred while in tension the variant with '*c* axis' is preferred.

therefore the ⟨0 0 1⟩ crystals subjected to tension will have their *c*-axis as vertical, [0 0 1], while the compression samples will have their *a*-axis as vertical, [1 0 0]. This is illustrated with the two schematics given as Fig. 6. The magnetization results on these biased variant samples are shown in Fig. 7. We note that the magnetization experiments are conducted at 50 K where the material is in the martensitic state. The compression loading biases the martensite variant with '*a*-axis' as vertical, and it is noted that the martensite in the [1 0 0] direction represents an easy axis (the upper curve). The role of deformation (0.5% and 1% strain) is small but not negligible. For comparison, the polycrystalline results are also-included (the lower curve). The polycrystalline samples had a grain size near 100 μm and crystallographic texture as described earlier.

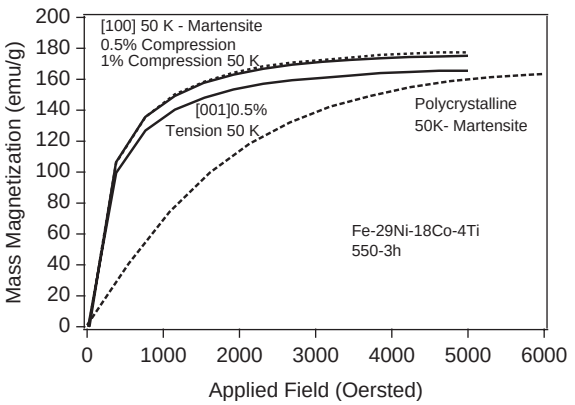

Fig. 7. The magnetization of [0 0 1] crystals with biased martensite variants and polycrystalline material in the martensitic state. The upper curves correspond to compression under 0.5% and 1% deformation respectively. The results show that the '*a*-axis' is the easy axis in FeNiCoTi.

The magnetization behavior of [0 1 1] and [1 2 3] crystals in the martensitic and austenitic regimes are shown in Fig. 8. No stress biasing was used for the single crystals and the results represent the rotation of the magnetization (and domain wall motion) associated with multiple variants in the martensitic regime (50 K results). We note that the saturation magnetization levels in the austenitic state (measured at 300 K) are lower compared to the martensitic state levels for both single crystals and polycrystalline cases. We also note that the [0 1 1] curve is between the easy and hard axis, indicating that *a*- and *c*- axis indeed represent the easy and hard axis, respectively. The [1 2 3] represents an unusual response displaying easier magnetization at low fields but crossing between the 'easy' and 'hard' axis curves at higher fields. The polycrystalline specimens (300 K austenite) were subjected to fields as high as 10 000 Oe and the saturation magnetization was not yet reached. The harder response of the polycrystalline samples is consistent with the [0 1 1] and [1 1 1] type texture measured earlier. The polycrystalline results show the need for very high applied fields to reach saturation, particularly when the crystals are

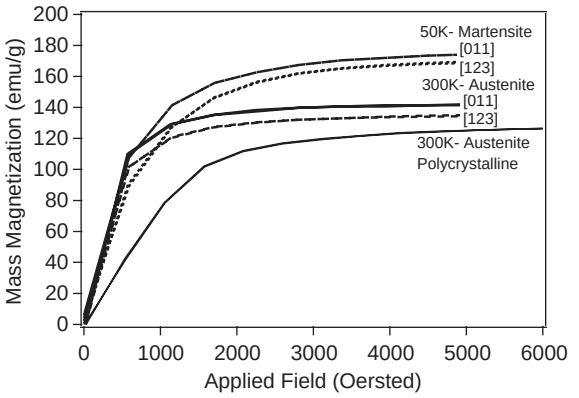

Fig. 8. The magnetization of [0 1 1] and [1 2 3] crystals and polycrystals.

preferentially oriented in [0 1 1] and [1 1 1] orientations. Overall, we note that the anisotropy in martensite is higher than in austenite, and this finding is consistent with results on other ferromagnetic shape memory alloys [10,15].

6. Discussion of results

6.1. Transformation hysteresis

The results confirm that the FeNiCoTi alloys undergo thermoelastic phase transformations associated with a change from the FCC to body centered tetragonal crystal structure. The austenite aging time influences the characteristic transformation temperatures, and the temperature hysteresis of the transformation. The transformation temperatures obtained through differential scanning calorimetry, thermal cycling experiments under stress, and magnetization behavior are in general agreement and point to maximum thermal hysteresis of nearly 135 °C. The transformation hysteresis is related to the amount of decrease in elastic energy of the martensite due to the relaxation of coherency stresses at the austenite/martensite interfaces. Evidence of such relaxation can be found in the form of dislocation loops at the martensite/austenite interfaces. Such a relaxation depends on the strength characteristics of the austenitic phases surrounding the martensite, the transformation shear magnitude associated with the martensite as well as the elastic modulus of the martensite domains. High slip resistance in austenite domains, a smaller transformation shear and lower modulus favor a lower thermal hysteresis in this class of alloys. A first-order estimate of transformation hysteresis can be obtained utilizing the free energy associated with the transformation as follows. The thermodynamics of diffusionless martensitic transformation has been expressed in terms of the following energies based on the work of Patoor et al., Gall and Sehitoglu [13,14]

$$\Psi(\Sigma_{ij}, T, f^n) = B(T_0 - T)\sum_n f^n + \frac{1}{2}\Sigma_{ij}C_{ijkl}\Sigma_{kl} + \Sigma_{ij}\sum_n \varepsilon^n_{ij} f^n + \frac{1}{2V}\int_\Omega \sigma^{\text{dist}}_{ij}\varepsilon^{\text{dist}-tr}_{ij}\,\mathrm{d}V, \quad (1)$$

where the first term represents the chemical free energy change, the second term is the overall strain energy stored in the system based on applied stresses, the third term represents the interaction energy between the applied stress and the transformation strain, and the last term is the elastic strain energy stored in the transforming domain. The f^n represents the volume fraction of nth variant of martensite. The transformation criteria is written as follows:

$$F^n = \frac{\partial\Psi}{\partial f^n} = B(T_0 - T^{A\to M}) + \Sigma_{ij}\varepsilon^n_{ij} - \sum_m H^{nm} f^m \geqslant F_c, \quad (2)$$

where the critical value of driving force F_c, is a material property. The last two terms represent the elastic strain energy. The first is associated with the interaction of the martensite variant with the surrounding domain, and the second term (the last term) is the strain energy of the martensite. This last term is expressed using the interaction matrix H^{nm}. The magnitude of terms in H^{nm} increases with shear modulus and also with the transformation shear strain. The term B in chemical free energy expression represents the entropy change between the two phases and can

be written as follows:

$$B = \rho \Delta s_0 = Q/T_0, \tag{3}$$

where Q is the latent heat produced during the transformation, ρ is the mass density and Δs_0 is the entropy change associated with the transformation. The latent heat produced by the transformation is the area enclosed by the heat flow (vertical axis of the DSC curve) over the transformation temperature. Note that $Q = (1/(\mathrm{d}T/\mathrm{d}t)) \int \frac{\mathrm{d}Q}{\mathrm{d}t}\, \mathrm{d}T$, where $\mathrm{d}T/\mathrm{d}t$ is the heating and cooling rate for the experiment. The range of integration is from the martensite start to martensite finish temperature. This integration provides the latent heat produced. Such an integration provides a Q value of 1.98×10^7 erg/g. The transformation temperature T_0, is the average of the two peaks (forward and reverse) given in the DSC curves. We note that Eq. (2) is able to predict the shift in transformation temperature as a function of applied stress (the Clausius–Clapeyron equation).

For reverse transformation a similar expression can be written,

$$F^n = \frac{\partial \Psi}{\partial f^n} = B(T_0 - T^{M\to A}) + \alpha \Sigma_{ij} \varepsilon_{ij}^n - \alpha^2 \sum_m H^{nm} f^m \geqslant F_c. \tag{4}$$

We are interested in thermal hysteresis $T^{M\to A} - T^{A\to M}$ associated with the transformation. The difference in elastic interaction energies between forward and reverse transformation can be ignored as a first approximation, then the thermal hysteresis for transforming materials can be written based on Eqs. (2) and (4) as,

$$\frac{Q}{T_0}(T^{M\to A} - T^{A\to M}) = \sum_m H^{nm} f^m (1-\alpha^2) - \Sigma_{ij} \varepsilon_{ij}^n (1-\alpha), \tag{5}$$

where α represents the amount of reduction in the internal energy associated with relaxation mechanisms such as due to dislocation generation at the interfaces. If $\alpha = 0$ the hysteresis would be very large while as α approaches 1 the transformation would proceed with zero thermal hysteresis. The second term on the r.h.s of Eq. (5) is smaller than the first term. These results confirm that the hysteresis response is strongly dependent on the non-chemical energy component which is the elastic stored energy within the martensite.

It is possible to estimate the amount of hysteresis based on Eq. (5) as follows. The transformation proceeds through the most favorably oriented martensite variant. The transformation shear for cubic to tetragonal transformation in FeNiCoTi is 0.1823. For the most favorably oriented variant we use a resolved shear stress factor of 0.5, consequently the unrelaxed transformation strain ε_{ij}^n, is approximately $\frac{0.1823}{2}$. The volume fraction of martensite corresponding to the hysteresis measurement corresponds to a value of $f = 0.5$. The value of the interaction matrix H^{nm} is a fraction of the shear modulus ($= \mu/400 = 67$ MPa) based on micro-mechanics considerations. Then we obtain $Q/T_0(T^{M\to A} - T^{A\to M}) = \{(67)(0.5)(1-\alpha^2) - (300)(.1823/2)(1-\alpha)\} \times 10^7$. The parameter Q/T_0 determined from the DSC results is $(1.98/266) \times 10^7$ erg/gK. The r.h.s of the above equality is in units of ergs/cm^3. The l.h.s is multipled by the density of FeNiCoTi material 7.962 g/cm^3 to obtain ergs/cm^3. Then, the predicted thermal hysteresis is of the order of 135 °C corresponding to an α value of 0.75.

The density of loops such as those shown in Fig. 3(b) dictate the degree of relaxation, α. The reduction of transformation strain (ε_1^n is the relaxed and ε^n is the unrelaxed transformation strain) occurs according to $\varepsilon_1^n = \varepsilon^n - NAb/6V$, where N is the number of dislocation loops; A is a geometric factor which is the dislocation loop area; b is the Burger's vector; and V is the volume of the single crystal martensite variant pair or CVP. The degree of relaxation of $1 - \alpha = NAb/6V\varepsilon^n$ depends on the number of loops produced. The volume of the martensite can be estimated from TEM results (such as those shown in Fig. 3(a)) where the thickness of the martensite variant is of the order of 500 nm. The width and length of the martensite plate is dictated by the specimen dimensions in the case of single crystals or the grain size in the case of polycrystals. Corresponding to a value of $\alpha = 0.75$, $A = 5 \times 10^{-4}$mm^2 $V = 1.5 \times 10^{-3}$mm^3, we obtain a first-order estimate of the number of loops as 1.4×10^6. The internal twinning spacing is of the order

300 nm (Fig. 3(b)). We then obtain, over a single martensite length of 3 mm, approximately 10^4 twins. If all of the relaxation occurred over a single variant, the corresponding number of loops per internal twin (shown in Fig. 3(b)) is predicted as 140. Since plastic dissipation occurs over a large number of martensite plates, the number of loops per internal twin will be much lower than 140. The measurement of the exact number of loops, and total dislocation densities is beyond the scope of this paper.

6.2. The role of magnetic fields and magnetic anisotropy

The shift in the transformation temperature with increasing magnetic field has been observed in this work (Fig. 5). This can be explained based on a simple thermodynamic treatment. In the presence of a magnetic field, the transformation criteria is modified as

$$F^n = \frac{\partial \Psi}{\partial f^n} = B(T_0 - T^{M\to A}) + (M_\alpha \operatorname{Cos}\theta_1 - M_\gamma \operatorname{Cos}\theta_2)I + \Sigma_{ij}\varepsilon^n_{ij} - \sum_m H^{nm} f^m \geqslant F_c, \quad (6)$$

where the M_α is the saturation magnetization for the martensitic phase, M_γ is the saturation magnetization for the austenitic phase, and I is the applied magnetic field. $\operatorname{Cos}\theta_1$ and $\operatorname{cos}\theta_2$ are the angle between the magnetic field and the easy axis of magnetization for a specific variant. In the case of multiple variants both of these quantities can be taken as 1 as a first approximation. In the presence of a magnetic field the nucleation criteria for martensite will be altered as follows:

$$\left\{-B + (M_\alpha - M_\gamma)\frac{\mathrm{d}I}{\mathrm{d}T}\right\}\sum_n f^n = 0 \text{ or } \frac{\mathrm{d}T}{\mathrm{d}I} = \frac{(M_\alpha - M_\gamma)T_0}{Q}, \quad (7)$$

where the $\mathrm{d}T/\mathrm{d}I$ is the rate of change of the transformation temperature with the applied magnetic field. The Q is known from thermodynamic DSC data as discussed above while T_0 is the average transformation temperature. Using $M_\alpha - M_\gamma = 35\,\mathrm{erg/G\,g}$, and a Q value of $1.98\times10^7\,\mathrm{erg/g}$. The shift in transformation temperature is estimated to be 14.1 K for a change in I of 3 T (30 000 G) is in general agreement with the experiments.

The ferromagnetic shape memory effect or field induced variant rearrangement producing high strains, has been observed in a number of transforming materials. These observations have been made in the martensitic regime. The nickel manganese gallium undergoes cubic to tetragonal transformation. Based on experiments the '*c*- axis ' is the easy axis in the nickel manganese gallium materials, and the '*a*'- axis is the hard axis. Upon application of the magnetic field normal to the '*c*-axis' the variant with the '*a*'- axis (long axis) is favored producing the highest strain change [10]. On the other hand, in the case of iron palladium alloys the '*a*'- axis is the easy direction and a magnetic field applied normal to the '*a*- axis' produces the highest strain change [15].

In an attempt to determine the magnetization behavior for selected martensite variants, we subjected specimens to tensile and compressive loadings in the martensitic regime and showed that '*a*-axis' of the martensite is the easy axis in this material (Fig. 7). This conclusion was reached by an indirect method of biasing the variants with prior deformation in the martensitic state. We note that there is no hysteresis associated with these curves indicating that the underlying processes are reversible. An application of strain of the order of 0.5% to 1% is sufficient to bring a single martensite variant based on the stress–strain response. This is known from extensive results by the authors on stress–strain response of these materials [1]. The degree of anisotropy in NiMnGa alloys is considerably higher compared to FeNiCoTi and FePd alloys. Clearly, further work is needed to optimize the microstructure to increase magnetic anisotropy. For example, the c/a ratio is highly sensitive to the aging treatment [2–3] and it is expected that larger c/a ratios could produce a larger dimensional change. At the same time very high c/a ratios ($c/a \gg 1$) could produce large transformation shear accompanied with plastic deformation. The plastic deformation could

limit the reversibility of transformation or rearrangement of the variants.

In the presence of a magnetic field, denoted as I, the magnetization in a domain could rotate and change direction to align with the applied magnetic field direction. Alternatively, under applied magnetic fields the domain walls can move to increase the volume fraction of the domain favorably oriented with respect to the applied field. It is noted that the application of a field changes the direction of magnetization in both cases, and the magnitude of the magnetization in each domain is at the saturation level denoted as M_s. In high magnetic anisotropy energy materials, such as ferromagnetic shape memory alloys, the energy required to move the boundaries is considerably less than the energy required to rotate the magnetization. The occurrence of boundary movement at relatively low magnetic fields is reversible and offers opportunities for designing new ferromagnetic shape memory materials. The present paper attempts to understand the role of applied stress on the biasing of martensite variants and the accompanied anisotropy of the magnetization. The results demonstrate differences in magnetization behavior between different martensite variants (Fig. 7) which is the basis for the magnetic shape memory effect.

Within the regime of applied magnetic field the curves have not reached their asymptotic limit (comparing 'a' axis versus 'c' axis and polycrystalline case). The major difference among these curves are expected at lower fields and this is depicted in this work. The magnetic anisotropy energy constant for martensitic FeNiCoTi can be evaluated as $\int_0^{M_s} I_{\text{Hard Axis}}(M)\,\mathrm{d}M - \int_0^{M_s} I_{\text{Easy Axis}}(M)\,\mathrm{d}M$ where the integrals represent the areas calculated (after curve fitting) associated with the easy and hard axis. In these calculations the magnetization is assumed to saturate at fields near 60 000 Oe. If the field at saturation was taken as 20 000 Oe the anisotropy constant changed by less than 2%. The magnetic anisotropy constant for FeNiCoTi was estimated as 8.34×10^5 ergs/cm^3 from the results (Fig. 7). The FeNiCoTi anisotropy constant value is lower than the 2.45×10^6 ergs/cm^3 value for Ni_2MnGa [10] and 3.2×10^6 ergs/cm^{3}for CoNiAl [16] but higher than the value of 3.4×10^5 ergs/cm^{3}for $Fe_{70}Pd_{30}$ [15].

The magnetization results demonstrated that the saturation magnetization in FeNiCoTi is near 165 and 130 emu/g in the martensitic and austenitic phases respectively. These results are in agreement with the reported levels on polycrystals by Hayashi et al. [11]. The magnetic field required for saturation is significantly higher in the polycrystalline samples compared with single crystals (Figs. 7 and 8). The presence of grain boundaries and lack of significant texture in the polycrystalline case is partially responsible for the very high magnetic fields required for saturation in the polycrystalline case.

7. Conclusions

(1) The results clearly demonstrate that the thermal hysteresis in FeNiCoTi is of the order of 135 °C. The thermal hysteresis in the FeNiCoTi alloys is linked to the relaxation of elastic strain energy due to dislocation formation at the austenite to martensite interfaces. A thermodynamics formulation is presented that provides theoretical predictions of thermal hysteresis in general agreement with the experimental results.

(2) The application of a magnetic field or stress shifts the transformation temperatures consistent with the thermodynamics of the transformation. This shift is less than 20 °C as the magnetic field is increased from 4 to 7 T in FeNiCoTi. The temperature shift is estimated as 14 K using the thermodynamics formulation presented in this study.

(3) A unique method of predeforming the samples in the martensitic state and biasing of the martensite variants was introduced. The magnetization behavior is crystal orientation and crystal structure dependent. The [1 0 0] direction (along a-axis) is the easy axis of magnetization compared to the [0 0 1] direction (along c-axis). The magnetic anisotropy energy constant was estimated as 8.34×10^5 ergs/cm^3 which is comparable to other ferromagnetic shape memory alloys.

(4) Further aging treatments and compositional changes can be devised to optimize this class of

alloys to achieve higher shape memory strains and higher magnetic anisotropy. These changes will alter the transformation temperatures and the c/a ratios which in turn dictate the overall magnetic and mechanical behaviors.

Acknowledgements

The work is partially supported by Air Force Office of Scientific Research, Directorate of Aerospace and Materials Sciences, Arlington, Virginia under Grant #F49620-01-1-0136, and also NSF Grants CMS-0332824 and CMS-0428428.

References

[1] H. Sehitoglu, X.Y. Zhang, T. Kotil, D. Canadinc, Y. Chumlyakov, H.J. Maier, Met. Mater. Trans. 33A (2002) 3661.
[2] V.V. Kokorin, V.V. Martynov, Fiz. Met. Metalloved. 9 (1991) 106.
[3] V.V. Kokorin, L.P. Gun'ko, O.M. Shevchenko, Phys. Met. Metall. 74 (5) (1992) 502.
[4] L.P. Gun'ko, V.V. Kokorin, O.M. Shevchenko, Phys. Met. Metall. 72 (4) (1991) 209.
[5] N. Jost, K. Escher, P. Donner, M. Sade, K. Halter, E. Hornbogen, Wire 40 (6) (1990) 639
See also N. Jost, Metallkd 44(1) (1990) 17.
[6] H. Kloss, Z. Metallkd 3 (1996) 175.
[7] T. Maki, in: K. Otsuka, C.M. Wayman (Eds.), Shape Memory Materials, Cambridge University Press, Cambridge, 1998 (Chapter 5).
[8] E. Cesari, V.A. Chernenko, V.V. Kokorin, J. Pons, C. Segui, Scripta Mater. 40 (3) (1999) 341.
[9] Y.N. Koval, V.V. Kokorin, L.G. Khandros, Phys. Met. Metall. 48 (6) (1979) 1309.
[10] R. Tickle, Ferromagnetic shape memory materials, Ph.D. Thesis, University of Minnesota, 2000.
[11] R. Hayashi, S.J. Murray, M. Marioni, S.M. Allen, R.C. O'Handley, Sensors Actuators 81 (2000) 219.
[12] J.S. Kallend, U.F. Kocks, A.D. Rollett, R.H. Wenk, Mater. Sci. Eng. A 132 (1991) 1.
[13] E. Patoor, E.N. Siredey, A. Eberhardt, M. Berveiller, J. Phys. III 5 (C8) (1995) 227.
[14] K. Gall, H. Sehitoglu, Int. J. Plasticity 15 (1999) 69.
[15] R.J. Cui, Ph.D. Thesis, U. Minnesota, 2002.
[16] A. Fujita, H. Morito, T. Kudo, K. Fukamichi, E. Kainuma, K. Ishida, K. Oikawa, Mater. Trans. JIM 44 (10) (2003) 2180.